ELSEVIER

Marine Geology 157 (1999) 47–68

MARINE GEOLOGY
INTERNATIONAL JOURNAL OF MARINE GEOLOGY, GEOCHEMISTRY AND GEOPHYSICS

Seismic stratigraphy of the Central Bransfield Basin (NW Antarctic Peninsula): interpretation of deposits and sedimentary processes in a glacio-marine environment

María José Prieto [a,*], Gemma Ercilla [b], Miquel Canals [a], Marc de Batist [c]

[a] *GRC Geociències Marines, Dpt. Geologia Dinàmica, Geofísica i Paleontologia, Universitat de Barcelona, Campus de Pedralbes, E-08071 Barcelona, Spain*

[b] *Dpt. de Geologia Marina i Oceanografia Física, Institut de Ciències del Mar (CSIC), Avda. Joan de Borbó s/n, E-08039 Barcelona, Spain*

[c] *Renard Centre of Marine Geology, University of Ghent, Krijgslaan 281 S8, B-9000 Ghent, Belgium*

Received 24 October 1997; revised version received 11 September 1998; accepted 1 October 1998

Abstract

The Central Bransfield Basin is a deep narrow trough between the northern tip of the Antarctic Peninsula and the South Shetland Islands. Analyses of single-channel, high-resolution seismic reflection data are used to characterise the seismic stratigraphy of the Central Bransfield Basin. The tectonised acoustic basement is overlain by a 1-s-thick sedimentary cover composed of two main sedimentary sequences. The Lower Sequence, which shows synsedimentary deformation, has only been identified on the Antarctic Peninsula margin. The Upper Sequence is a complex sedimentary package composed of eight seismic units whose distribution, geometry and seismic facies allow two types of seismic units to be distinguished: slope and basinal units. The slope units, constituted by progradational stratified seismic facies, form a sedimentary wedge extending from the shelf edge. The basinal units fill the basin floor showing chaotic and undulated seismic facies that change basinward into stratified seismic facies. Both types of seismic units display an interfingering pattern at the base of the slope, suggesting an alternating shift of the sedimentary depocentre, from the slope to the basinfloor and vice versa. This alternate pattern indicates that the sedimentary processes responsible for the infilling of the Central Bransfield Basin followed a cyclic pattern, which has likely been associated with the advance and retreat of the ice sheets over the margins during glacial and interglacial episodes. During glacial periods, the ice sheets advanced, eroded the shallower sea floor areas and deposited diamicton and debris flow deposits along the moving grounding line, resulting in a progradational sedimentary wedge on the slope. At the end of glacial periods, coinciding with the retreat of the ice sheets, extensive sediment failures affected the continental margin. During interglacial periods the ice sheets remained restricted to coastal locations and glacial troughs, where processes of meltwater formation might have been significant. Sediment-laden underflows are generated within these troughs, from where they flow and spread over the shelf and down the slope to the basinfloor as sediment gravity flow deposits. The combined effect of these processes is a progradational build up of the shelf and an aggradational infilling of the basin floor, together with the development of the interfingering pattern at the base of the slope.

Keywords: glacio-marine sedimentation; seismic stratigraphy; Central Bransfield Basin; glaciated margins

* Corresponding author. Tel: +34 3 4021375; Fax: +34 3 4021340; E-mail: mjose@beagle.geo.ub.es

0025-3227/99/$ – see front matter
PII: S0025-3227(98)00149-2

1. Introduction

The Central Bransfield Basin (CBB) is a Cenozoic marginal basin located between the Antarctic Peninsula (AP) and the South Shetland Islands (SSI), Antarctica (Fig. 1). The CBB is separated from the Western and Eastern Bransfield Basins by two highs formed by Deception and Bridgeman Islands, respectively. During the past decades, the CBB has been the object of various geological and geophysical studies. These studies provided new data relevant to the basin's formation and geodynamic evolution (Gamboa and Maldonado, 1990; Grad et al., 1992; Henriet et al., 1992; Barker and Austin, 1994; Lawver et al., 1995). Most of these surveys have focused on the deep structure of the basin and little attention has been paid to the detailed stratigraphy of the basin's sedimentary infill. Only Jeffers and Anderson (1990) and Banfield and Anderson (1995) studied the fine-scale seismic stratigraphy of the CBB using intermediate-resolution reflection seismic data. In the present study, we aim to contribute to this work by interpreting the sedimentary architecture and the stratal geometry patterns from seismic-stratigraphic analyses of single-channel, high-resolution seismic reflection profiles. We also propose a depositional model that relates the observed morphologic features, seismic facies, stratal and growth patterns to the geodynamics of the CBB and to its glacio-marine sedimentary setting. Our study focuses on slope and basin physiographic provinces, since it is here that seismic-stratigraphic units reached their maximum thickness. For reasons of simplicity we refer to these two provinces together as CBB.

2. Geological setting

The Pacific margin of the AP was a collision margin during the Mesozoic and Cenozoic (Barker, 1982). Along the South Shetland Trench, subduction stopped or decreased to a slow rate about 4 Ma ago, when spreading ceased at the segment of the Antarctic–Phoenix ridge between the Hero and Shackleton Fracture Zones (Fig. 1a). The opening of the Bransfield Basin (BB) has been dated between 4 and 1.3 Ma (Barker and Dalziel, 1983). It probably resulted from the mechanism of roll-back, following the cessation of subduction, and from the extensional stress induced in the AP continental crust (Barker, 1982; Barker and Dalziel, 1983; Lawver et al., 1995).

The present-day CBB is an asymmetric trough characterised by a steep rectilinear SSI margin, a gentle sinuous AP margin and an almost flat basin floor disrupted by volcanic edifices. These volcanoes form a discontinuous lineament along the basin axis where they depict an incipient seafloor spreading ridge (Gràcia et al., 1996, 1997). Seismic and volcanic activity (Pelayo and Wiens, 1989), high heat flow (Nagihara and Lawver, 1989), a positive magnetic anomaly (Roach, 1978; Gràcia et al., 1996) and a large negative gravity anomaly (Garret, 1990) have been reported in the CBB, supporting the idea that it is a young, active rift basin (Saunders and Tarney, 1984; Fisk, 1990; Grad et al., 1992; Lawver et al., 1995).

Seismic reflection data collected in the CBB in recent years have allowed the recognition of the acoustic basement distinct from the sedimentary cover (Gamboa and Maldonado, 1990; Jeffers and Anderson, 1990; Acosta et al., 1992; Henriet et al., 1992; Barker and Austin, 1994; Banfield and Anderson, 1995; Gràcia et al., 1996). The acoustic basement in the basin axis is generally believed to be composed of thinned continental crust intruded by dykes (Ashcroft, 1972; Birkenmajer, 1992; Grad et al., 1992), and volcanic materials, all related to the extension along the basin axis (Barker and Austin, 1995). In the AP margin, the acoustic basement probably consists of metasediments and metavolcanics that are laterally equivalent to the sedimentary series defined onshore (Smellie, 1984), and are believed to correspond to the infilling of a previous marginal basin (Gamboa and Maldonado, 1990; Barker and Austin, 1995; Prieto et al., 1997). In fact, the Trinity Peninsula Group in the AP, and the Myers Bluff Formation in the SSI show similar sedimentologic and structural characteristics which hint at a same origin in a backarc basin (Aitkenhead, 1975; Hyden and Tanner, 1981; Smellie, 1984). The acoustic basement is arranged in blocks, rotated along normal faults created by the stretching and break up of the former AP and marginal basin (Gamboa and Maldonado, 1990; Jeffers and Anderson, 1990; Acosta et al., 1992).

The acoustic basement is overlain by a sedimentary cover with a thickness of 700–1000 ms

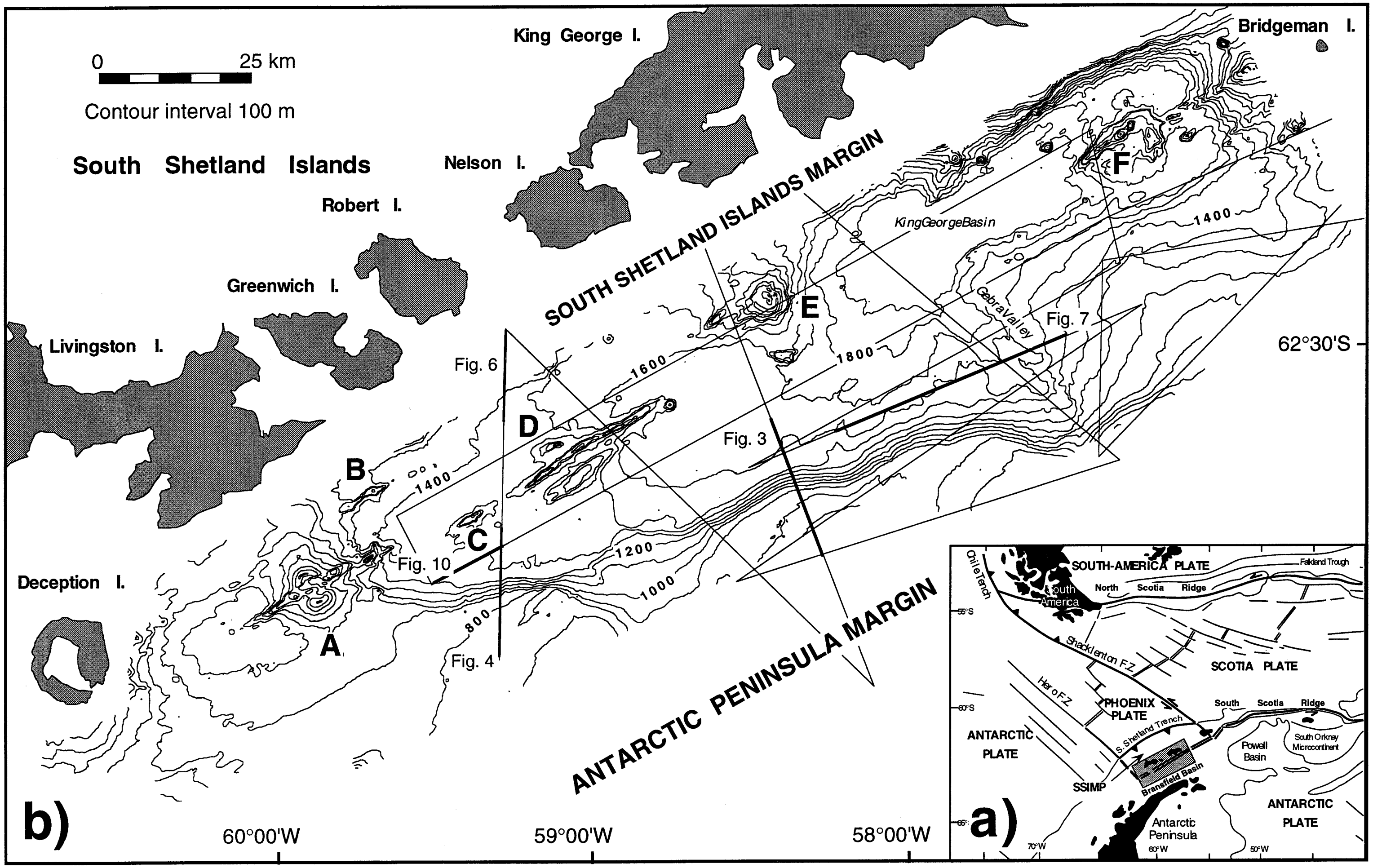

Fig. 1. (a) Geodynamic setting of the Bransfield Basin. *SSIMP*: South Shetland Islands Microplate. (b) Bathymetric map of the Central Bransfield Basin, with location of seismic lines recorded during the Gebra'93 cruise. Labels A to F indicate the location of the six large volcanic edifices (modified from Gràcia et al., 1996). Thick lines show the location of the seismic lines in Figs. 3, 4, 6, 7 and 10.

TWTT formed during two major sedimentary sequences separated by a regional unconformity. The Lower Sequence fills an older graben system and is faulted and occasionally tilted towards the continent (Gamboa and Maldonado, 1990; Prieto et al., 1997). The Upper Sequence is less tectonised and controls the present morphology of the AP margin. The Lower Sequence, or 'rift sequence', has been attributed to the rift stage during which the AP margin was formed. The Upper Sequence, or 'drift sequence', contains internal erosional unconformities and has been attributed to glacio-marine sedimentary processes induced by the advances and retreats of the Antarctic ice sheet during the Plio–Quaternary glacial periods (Anderson et al., 1983; Jeffers and Anderson, 1990; Henriet et al., 1992; Banfield and Anderson, 1995).

3. Data base and methodology

A grid, corresponding to 16 lines of single-channel, high-resolution seismic reflection data, with a total length of about 1100 km, was collected in the CBB (Fig. 1b). The seismic source was a 2.9 l Bolt 1500 C airgun. The reflected signals were detected with a SIG 120 three-channel streamer with an active section of 150 m. The data were recorded digitally with the Elics Delph2 high-resolution acquisition system. Post-acquisition data processing, including bandpass-filtering, deco-filtering and scaling, was carried out on both the Delph2 and the Phoenix Vector processing systems. The vertical resolution of the processed data was about 5 ms and penetration was often in excess of 1 s TWTT.

Across-basin profiles (trending approximately NNW–SSE) cross the slope of the AP continental margin, the basin floor, some of the central seamounts and segments of the steep narrow SSI slope. These profiles allow the comparison of both margins and their influence in the sedimentary supply to the basin. Along-basin profiles (trending approximately ENE–WSW) cross part of the AP slope and the central basin floor. These profiles allow us to recognise the seismic sequences and seismic units that built the AP margin and filled the basin floor, and to investigate their spatial and temporal variations. We have correlated unconformity-bounded seismic units across the whole seismic grid. Furthermore, the analysis of the main features (boundaries, internal configuration, geometry, thickness) of these seismic units has allowed us to interpret depositional processes and how the basin infilling has evolved to its present configuration.

Swath bathymetry data were acquired over an area of 10 000 km^2 using the combined SIMRAD EM-12/EM-1000 system. The data set fully covers the AP continental margin from the upper slope down to the basin floor and the slope of the SSI margin, between Bridgeman and King George Islands (Gràcia et al., 1996) (Fig. 1b).

4. Morphology

The CBB is a NE–SW-trending basin, 230 km long, 130 km wide and 1950 m deep. The swath bathymetry map of the CBB (Gràcia et al., 1996, 1997) provides a useful tool to recognise the physiographic elements and the main morphosedimentary features (Fig. 2). This map does not cover the AP and SSI shelves, and to characterise these areas we used a compilation of pre-existing single-beam bathymetry data (Lawver et al., 1995). A later map by Lawver et al. (1996) covers additional segments of the SSI slope.

The AP margin has an irregular shelf, about 60 km wide and 200 m deep. It is deeply incised by four troughs, that run slightly oblique to nearly perpendicular to the margin: the Orleans Trough in the southwest, Antarctic Sound in the northeast and two unnamed troughs in between (Fig. 2). The troughs have U-shaped cross-sections, which suggests that they are glacially scoured features (Jeffers and Anderson, 1990). The AP slope shows two platforms or terraces at different depths, giving the margin a step-like morphology. A wide (10–15 km) wavy upper platform (Jeffers and Anderson, 1990; Acosta et al., 1992) is situated between 600 and 800 m. It is slightly tilted towards the basin (0.6–2.4%) and only slightly incised by the glacial troughs. The lower platform lies at a depth between 1000 and 1400 m. It is a discontinuous feature, 20–35 km wide, with a conspicuous convex shape that dips gently (3%) towards the basin. This platform connects basinward with a steep (8%) lower slope that abruptly termi-

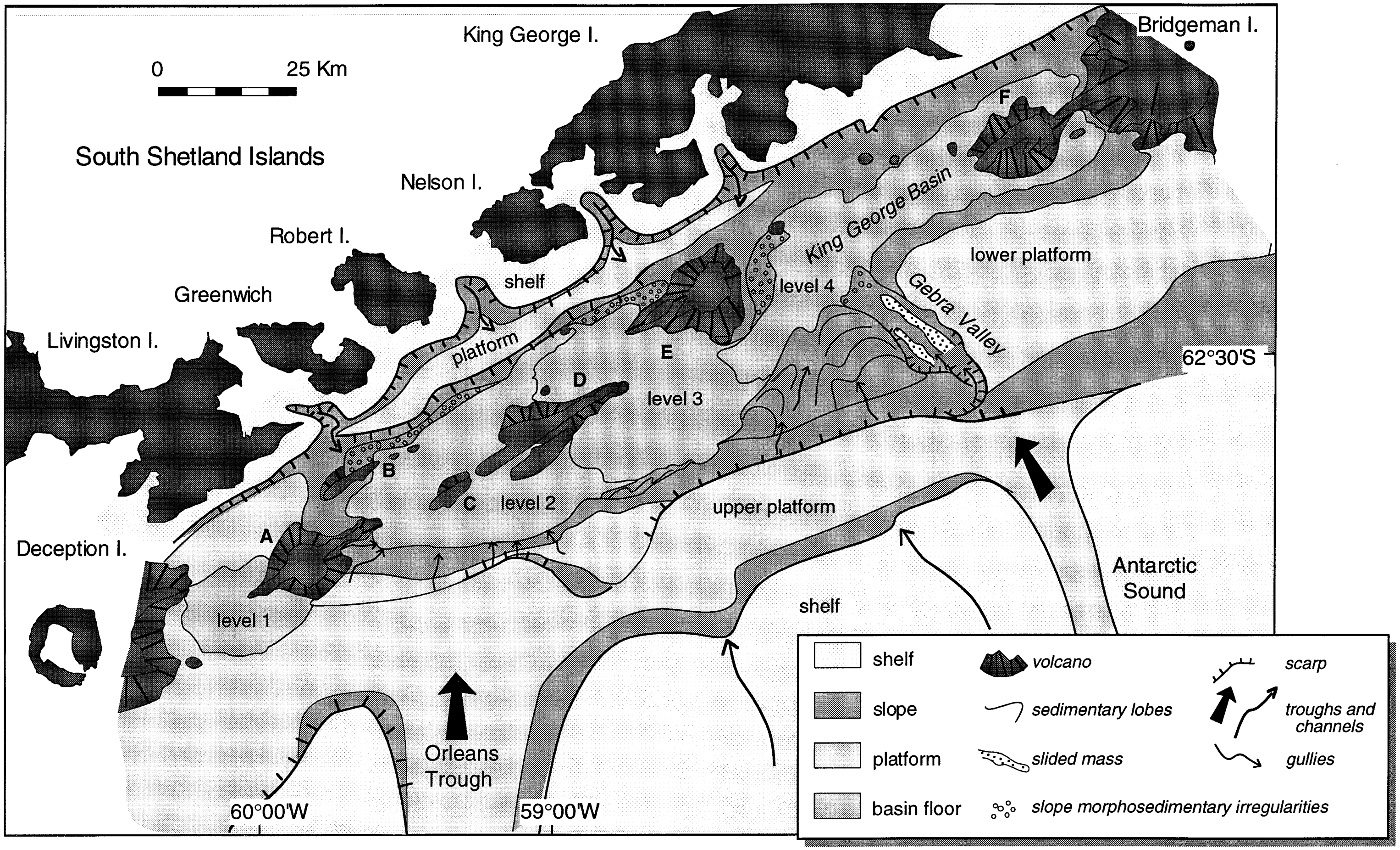

Fig. 2. Morphosedimentary map of the Central Bransfield Basin. To characterise the SSI margin, a compilation of pre-existing single-beam bathymetry data has been used (Lawver et al., 1995).

nates at the basin floor. Where the lower platform is not present, the slope is much steeper (up to 18%).

The AP margin is indented by submarine valleys (Fig. 2). A large U-shaped valley, named Gebra Valley, was identified by Canals et al. (1994) in the northeastern half of the AP margin (57º45, 63º30) (Fig. 1b and Fig. 2). Gebra Valley is 30 km long, 6 km wide and extends from depths of 800 to 1900 m on the basin floor. Its flanks are 200 m high and the generally flat bottom is marked by irregularities which might be interpreted as mass gravity flow deposits. The head of the valley is formed by several semicircular and steep scarps (8%), the morphology of which resembles that of active slide scars (Fig. 1b and Fig. 2). On the southwestern half of the AP margin, several 10–15-km long gullies incise the slope. They have a U-shaped cross-section, and reach widths of up to 2 km and depths of up to 40 m.

The rectilinear SSI margin is characterised by a narrow shelf (5 km) up to 200 m deep, where a scarp extends down to the steep slope. The shelf is incised by short troughs developed between the islands and at the mouth of the bays and fjords of the islands. They also cut the slope until reaching a flat, 700 m deep platform, in front of Greenwich and King George Islands. This platform has not been identified in front of Livingston and King George Islands, where the slope is a continuous feature from the shelf break to the basin floor (Lawver et al., 1995) (Fig. 2). The slope shows the highest dip, up to 26%, in front of King George Island. The foot of the slope shows small depositional irregularities.

The basin floor of the CBB is a relatively narrow ($<$30 km wide), flat trough. It shows four bathymetric levels that progressively deepen the sea floor from 1000 to 1950 m, from the southwest to the northeast. The deepest level constitutes the King George Basin, a very flat, 20 km-wide and 50-km long basin (Fig. 1b and Fig. 2). Six large volcanic edifices, with different morphologies (labelled from A to F in Fig. 2) rise above the seafloor (Gràcia et al., 1996). Altogether, they form a discontinuous lineament that extends from Deception to Bridgeman Islands. This lineament divides the basin floor into two halves or subbasins: a northern subbasin, between the SSI margin and the volcanic lineament, and a southern subbasin, between the lineament and the AP margin. In addition to the large volcanic edifices, small cone-shaped volcanoes appear scattered between the axial lineament and the SSI margin (Figs. 1 and 2).

5. Acoustic basement of the Central Bransfield Basin

The acoustic basement has been identified at different depths in the CBB. It crops out at the seafloor at the AP and SSI margins, at a depth of around 600 m, whereas in the basin floor it is covered by a sedimentary cover up to 1 s TWTT, and has been identified at a maximum depth of 3.2 s TWTT. The basement is everywhere tectonised. From both margins, normal faults deepen the basement basinward, defining the axial trough where the basin is located. The seismic character of the basement varies across the basin. At the margins the basement is composed of stratified and largely continuous reflections, suggesting a sedimentary character (Fig. 3). In contrast, on the basin floor the basement shows a chaotic seismic character with its top formed by a strongly reflective surface. This suggests a direct relation with the axial volcanic edifices and volcanic intrusions of the CBB. The top of this ‘crystalline’ basement can be traced for 15 km from the volcanic edifices, either forming the seafloor or as a highly reflective continuous surface below the sedimentary cover.

6. The sedimentary cover in the Central Bransfield Basin

The overall seismic stratigraphy of the CBB consists of a complex package of sedimentary sequences and units that overlies the acoustic basement. Two major sedimentary sequences have been identified within this sedimentary cover: the Lower Sequence and Upper Sequence (Fig. 3).

6.1. The Lower Sequence

The Lower Sequence (LS) has only been recognised in the AP margin, where it directly overlies the sedimentary basement. It extends from the upper platform (1.5 s TWTT deep) to the base of the slope and the central basin floor (3.2 s TWTT deep). The LS onlaps the basement onshore, and downlaps it

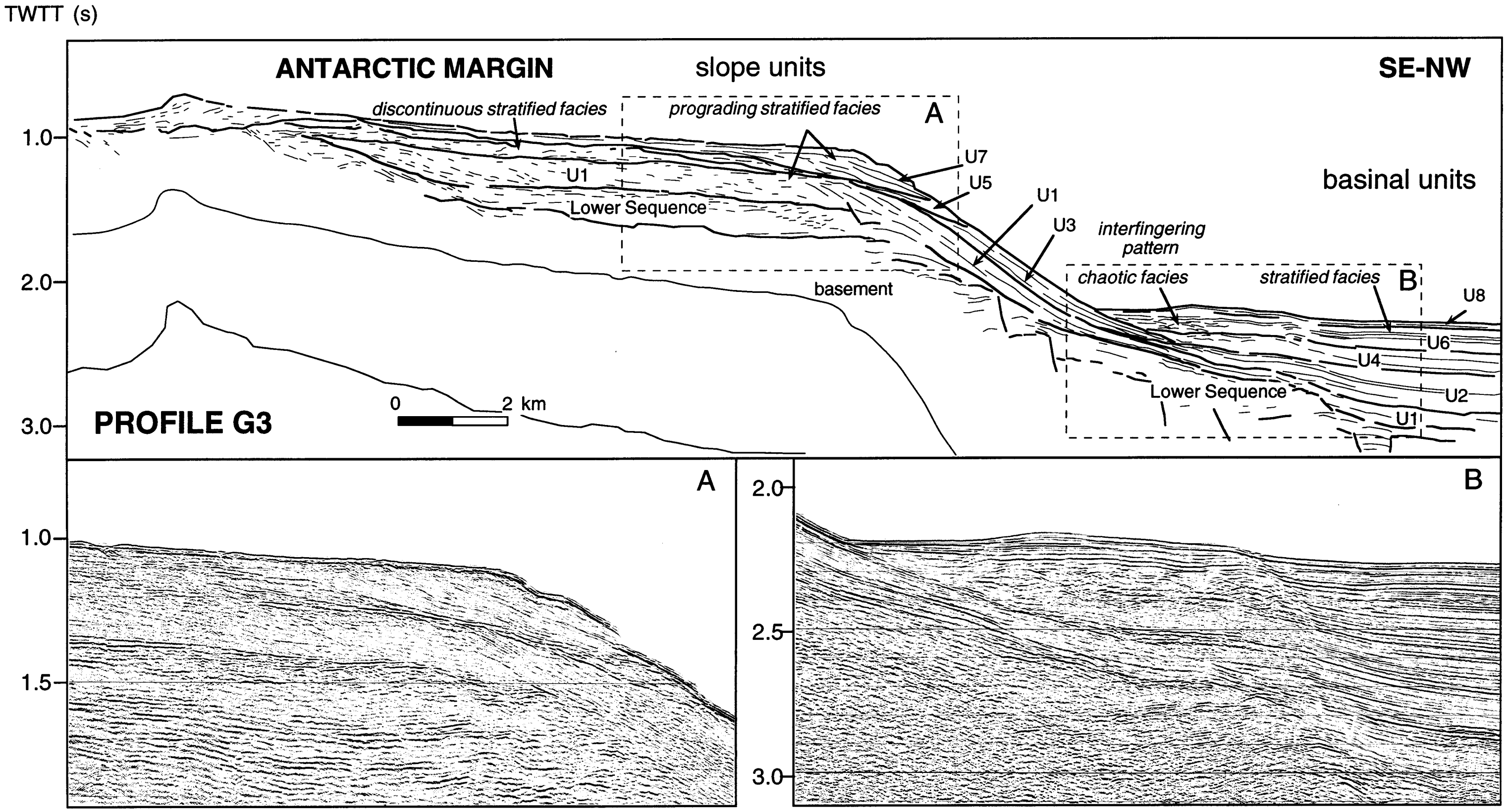

Fig. 3. Interpreted line drawing of seismic line G3 showing the distribution of the slope (U1, U3, U5 and U7) and basinal units (U2, U4, U6 and U8). Two details of this seismic line show the prograding stratified facies and interfingering pattern at the foot of the Antarctic Peninsula slope. Location of the seismic line is shown in Fig. 1b.

offshore (Fig. 3). The top of the LS is a widespread erosional surface identifiable throughout the AP margin (Fig. 3). The LS forms a faulted, slightly deformed sedimentary wedge, composed of discontinuous stratified facies with several configurations: parallel, progradational, and divergent. The parallel configuration occurs on the upper platform, the progradational facies on the slope and the divergent facies at the base of slope, in the vicinity of normal faults, suggesting synsedimentary deformation. Landward dipping (4º) reflections have also been recognised at the base of the slope, probably related to basement blocks tilted along normal faults (Fig. 3). The main depocentres of the LS are located at the base of the AP margin and range from 0.15 to 0.25 s.

6.2. The Upper Sequence

The Upper Sequence (US) is composed of eight sedimentary units, labelled 1 to 8, from bottom to top. We have defined two types of sedimentary units based on their distribution: slope units (U1, U3, U5 and U7) and basin-floor units (U2, U4, U6 and U8). The four slope units are observed in the AP margin. Only units U3, U5 and U7 have been identified in the SSI margin. The basin-floor units (U2, U4, U6 and U8), and their subunits, are located in the central basin floor. Slope and basinal units interfinger at the base of the slope.

6.2.1. Slope units

Unit 1 (U1), the oldest sedimentary unit of the Upper Sequence, has only been identified on the AP margin, where it extends from the upper platform to the basin floor of the southern subbasin (Figs. 3 and 4). Along the whole margin, U1 is composed of progradational stratified seismic facies with high-angle (7–10º) dipping reflections that downlap onto the LS basinward and onlap the basement landward (Figs. 3 and 4). The top of the unit is an erosional surface in the upper platform, changing to a conformable surface basinward (Fig. 3). The thickness of U1 ranges between 0.25 and 0.35 s TWTT, and the main depocentres are located on the upper platform (Fig. 5a). U1 shows minor internal unconformities on the upper platform, adjacent to the Orleans Trough (Figs. 2 and 4).

Unit 3 (U3) has been identified in the AP margin. It overlies U1 on the upper platform and Unit 2 (U2) at the base of the slope (Fig. 3). The lower boundary of U3 is a downlap surface along the whole margin, and the upper boundary is an erosional surface on the upper platform, which becomes more conspicuous in the western sector of the AP margin (Fig. 4). This erosional surface changes basinward becoming conformable, locally outcropping on the slope (Fig. 3). The seismic facies of this unit is progradational stratified with very low-angle (1º) dipping reflections on the upper platform which become steeper (10º) towards the slope. The main depocentres of U3 are located within the upper platform, and their thickness ranges from 0.15 to 0.2 s TWTT (Fig. 5b). This unit also seems to be present in the SSI margin, where a 0.1–0.2 s TWTT thick sedimentary wedge overlies the basement (Fig. 6). It occupies the same stratigraphic level as U3 on the AP margin (i.e. below Unit 4 on the basinfloor and below Unit 5 on the slope). This would suggest that either the two are equivalent or the one at the SSI margin is older. The U3 equivalent wedge at the SSI margin is composed of the discontinuous progradational stratified seismic facies, and is bounded at the bottom by a downlap surface and at the top by an erosional surface.

Unit 5 (U5) occurs within the AP and SSI margins (Figs. 4 and 6). On both margins U5 overlies U3, and part of U4 at the foot of both slopes. The base of U5 is a downlap surface and the top is an erosional surface; both surfaces extend along the entire margin (Fig. 4). U5 shows discontinuous progradational stratified seismic facies, with very low-angle (1º) dipping reflections on the upper platform and higher-angle (6º) dipping reflections downslope (Fig. 4). U5 constitutes an irregular wedge, partly eroded, on the platform. It thins progressively until it pinches out both landward and basinward. The maximum thickness of the unit is 0.15 s TWTT at the AP margin and 0.1 s TWTT at the SSI margin (Fig. 5c).

Unit 7 (U7) is the youngest unit on the slope at both margins. Along the AP margin, it constitutes a sedimentary wedge on top of the platform edge, which is continuous along the whole margin (Figs. 3, 4 and 6). This wedge is particularly well developed at the southwestern sector of the AP margin, facing the mouth of Orleans Trough, where it mostly reaches the basin floor (Fig. 4). It overlies U5 at the platform, and part of Unit 6 (U6) at the foot of the

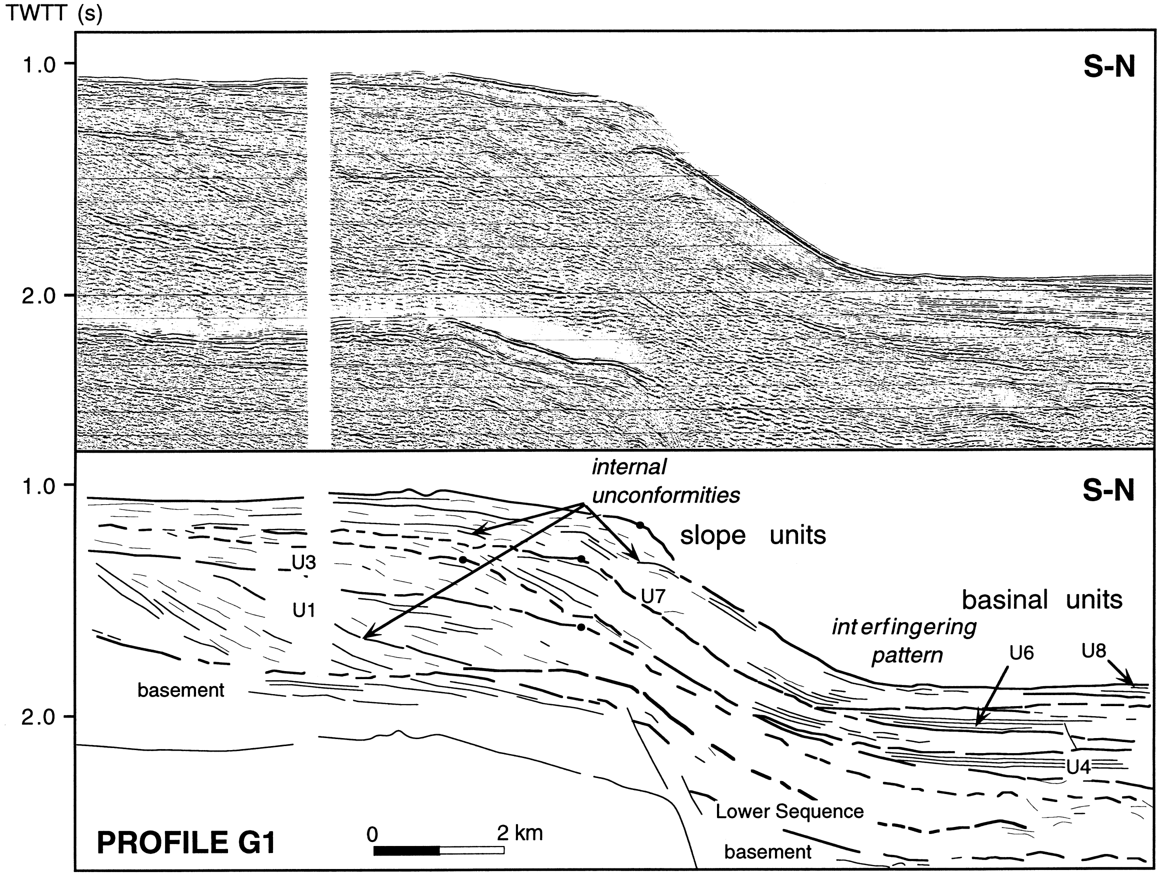

Fig. 4. Seismic line G1 and interpreted line drawing showing the distribution of the slope and basinal seismic units. Location of the seismic line is shown in Fig. 1b. Dots indicate the position of the platform edge at the end of sedimentation of each slope unit.

slope. Its base is a downlap surface, and its top coincides with the sea floor on the upper platform, where it is mainly conformable although locally erosional relief of about 30 m deep and 1 km wide can be identified. At the mouth of the Orleans Trough, where U7 reaches the base of the slope, its top is an erosional surface with incisions about 50 m deep and 1 km wide. U7 is characterised by progradational stratified seismic facies of very low-angle (1.5º) dipping reflections in the upper platform and more steeply inclined reflectors (4–8º) beneath the slope (Figs. 3 and 6). Additionally, we have also observed within U7 semitransparent chaotic seismic facies at the head of the Gebra Valley, and a 50 m high depositional mound with landward-dipping reflections (2.6º) in the AP margin (Fig. 3). The thickness of the unit ranges from 0.15 to 0.2 s TWTT (Fig. 5d).

6.2.2. Basinal units

Unit 2 (U2) only occurs in the central and easternmost sectors of the southern subbasin, between the AP margin and the axial volcanic lineament, here defined by volcanoes D and E (Fig. 1b). U2 overlies U1 at the foot of the AP margin, while further down into the basin it directly overlies a rough basement (Fig. 3). The top of U2 is a subhorizontal conformable surface, although locally, there is evidence of strong erosion, i.e. in the vicinity of volcanic edifice D. A minor discontinuity within U2 allows two subunits to be identified: a lens-shape lower subunit and a subtabular upper subunit. Several seismic facies appear within U2. Seismically chaotic subtabular interstratified depositional bodies with erosional bases occur at the foot of the slope and on the basin floor in front of the Gebra Valley

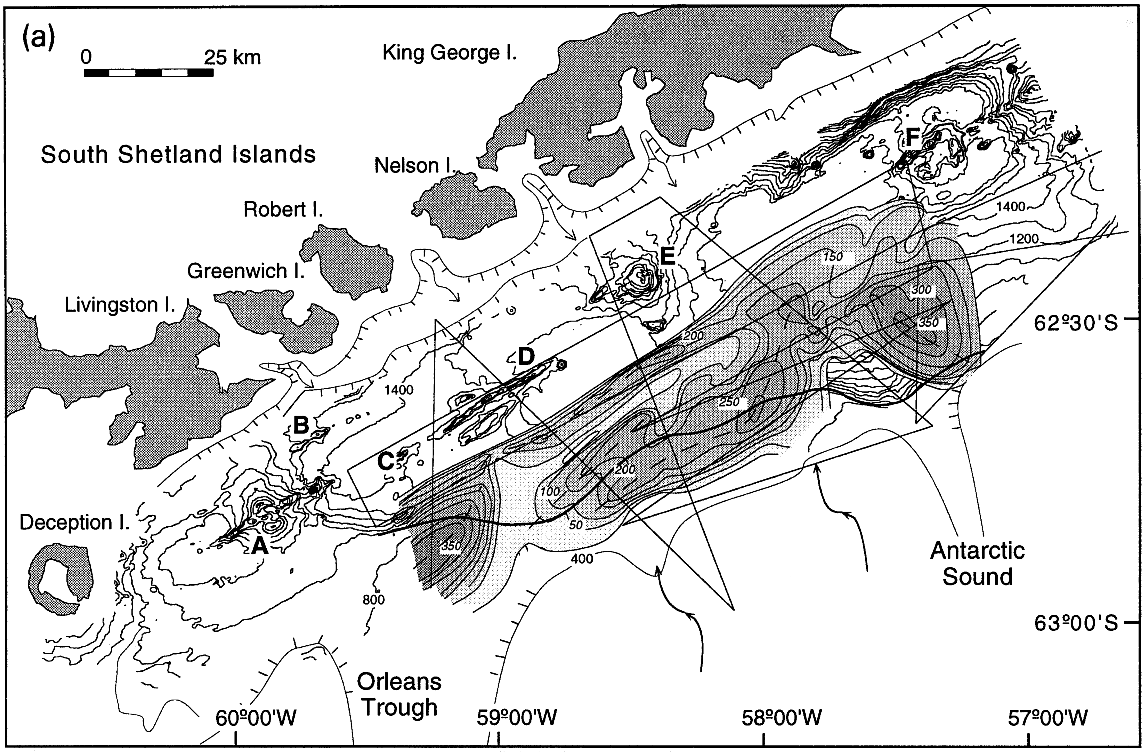

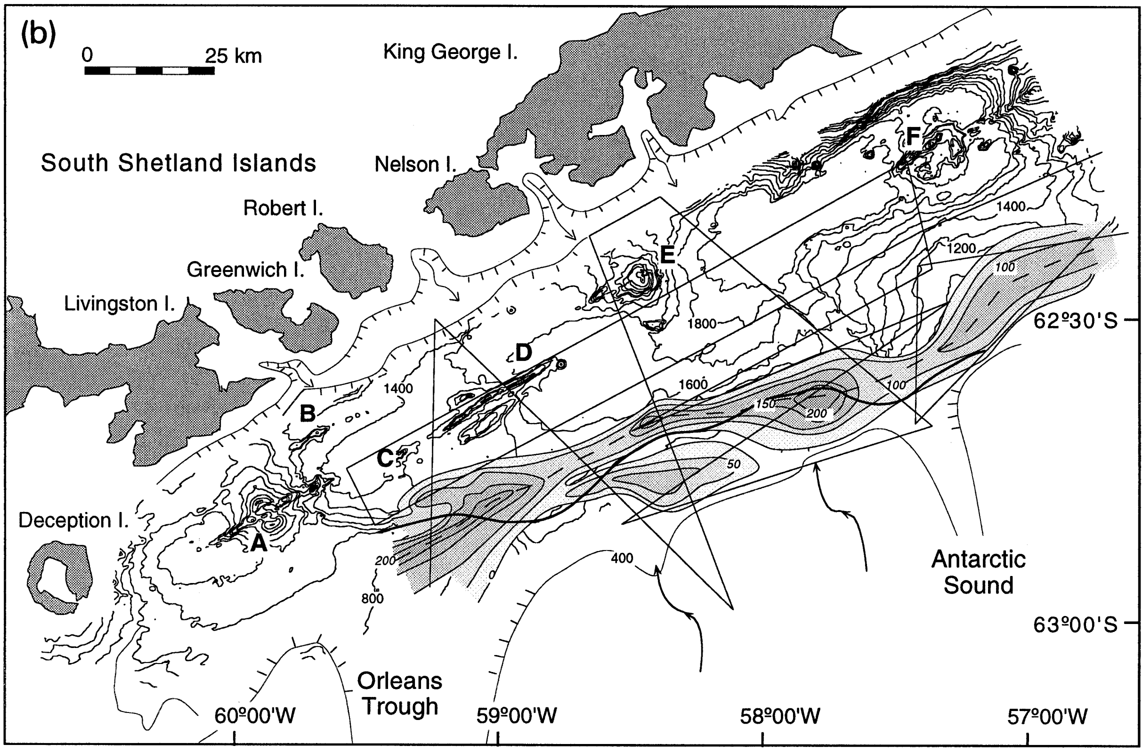

Fig. 5. (a,b,c,d) Isopach maps of the slope units U1, U3, U5 and U7 at the Antarctic Peninsula margin. Dashed line depicts the maximum thickness of depocentres and thick line marks the present day slope break. Contour interval 50 ms.

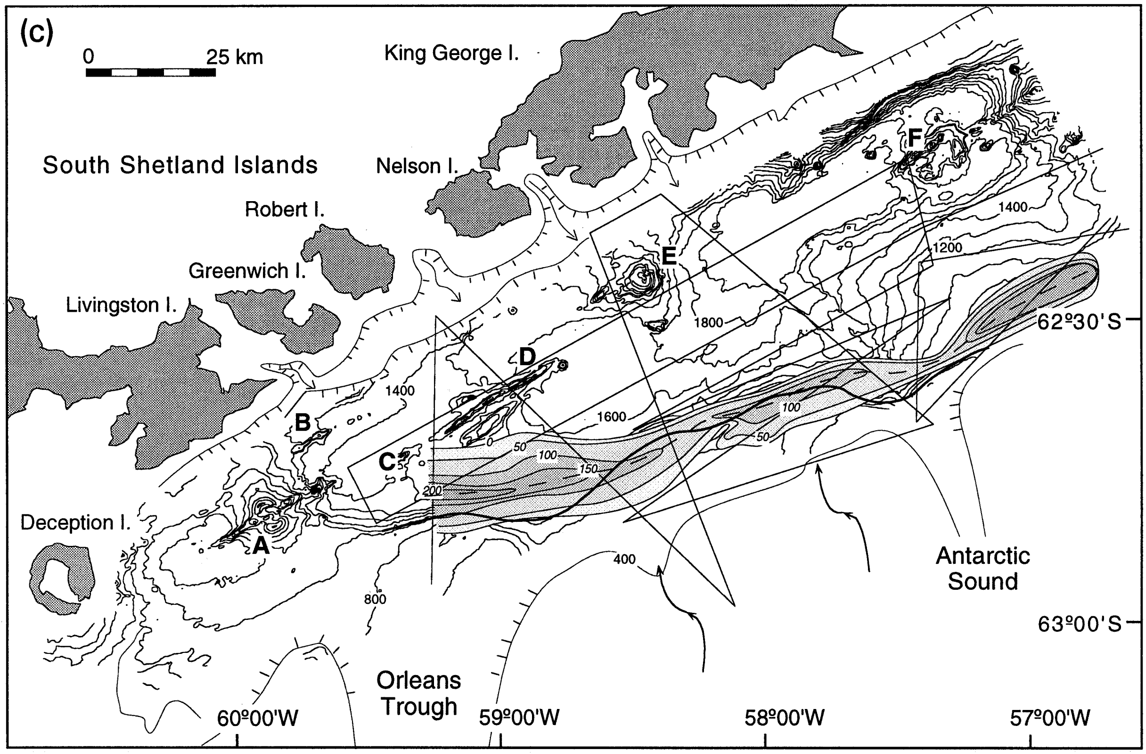

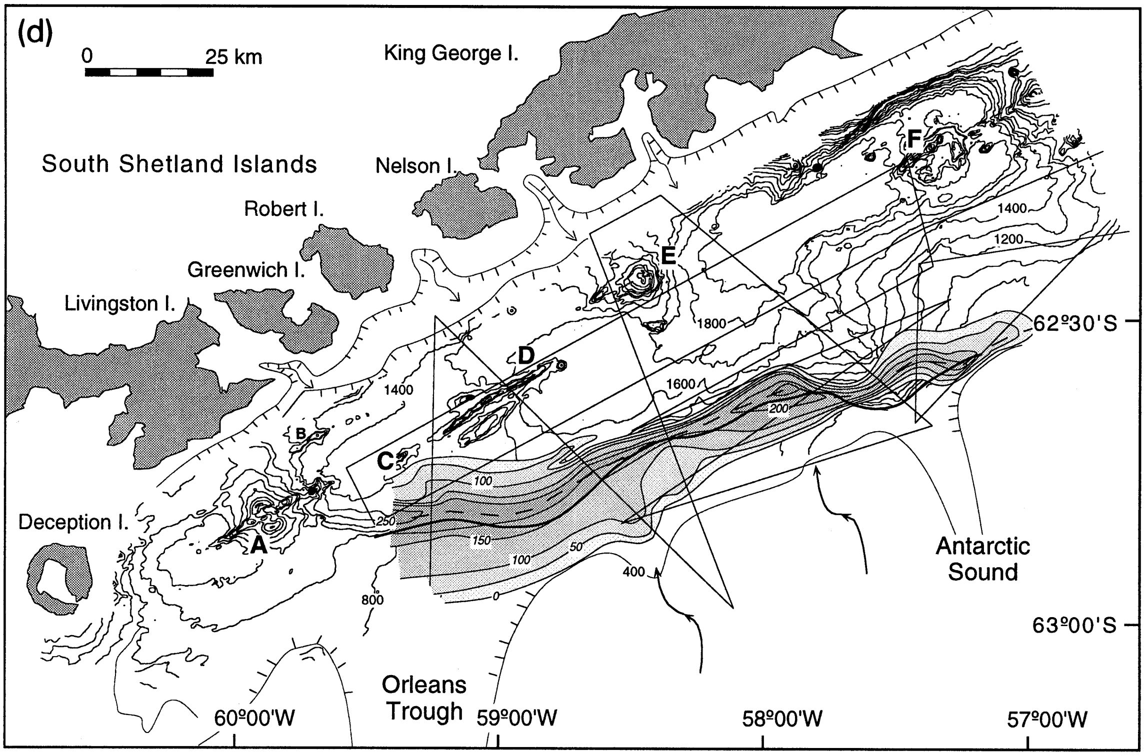

Fig. 5 (continued).

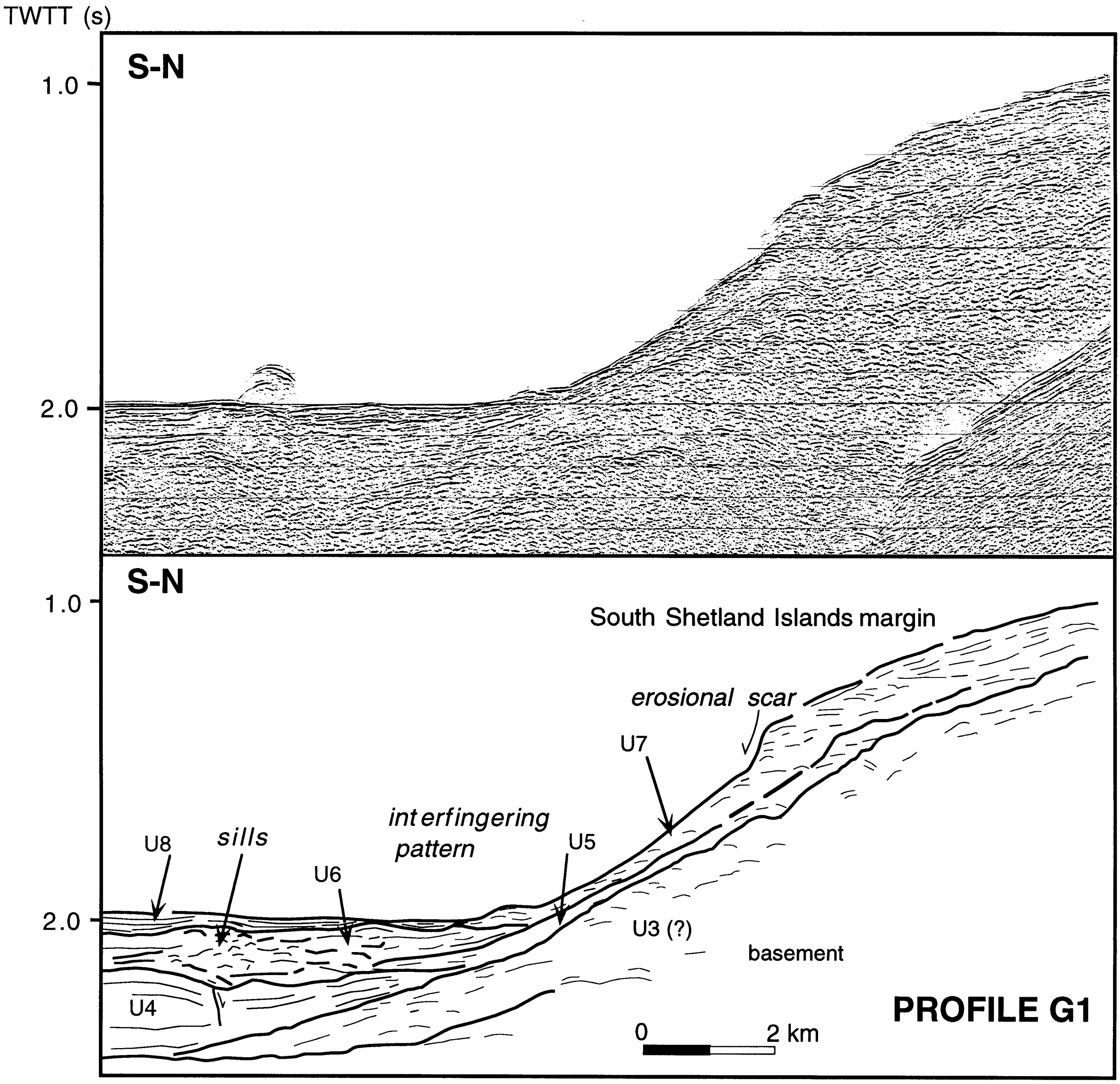

Fig. 6. Seismic line G1 and interpreted line drawing showing the slope units (U3, U5 and U7) identified at the South Shetland Island margin, and the basinal units (U4, U6 and U8) interfingering at the base of the slope. Location of the seismic line in Fig. 1b.

(Fig. 3). Basinwards, the dominant seismic facies is discontinuously stratified (Fig. 3). The thickness of U2 depocentres ranges between 0.2 and 0.3 s TWTT, thinning towards the AP margin, until it disappears.

Unit 4 (U4) overlies U3 at the base of the AP slope, overlies U2 between the AP margin and the axial volcanoes in the southern subbasin, and overlies the basement in the northern subbasin (Fig. 6). Both base and top of U4 are conformable surfaces. However, where the top of U4 crops out at the seafloor it becomes an irregular surface, with mounds and gentle erosional depressions as observed at the foot of the AP slope (Fig. 7). An internal unconformity allows us to divide U4 into two subunits with different seismic facies and spatial distribution. The lower subunit is restricted to the southern subbasin,

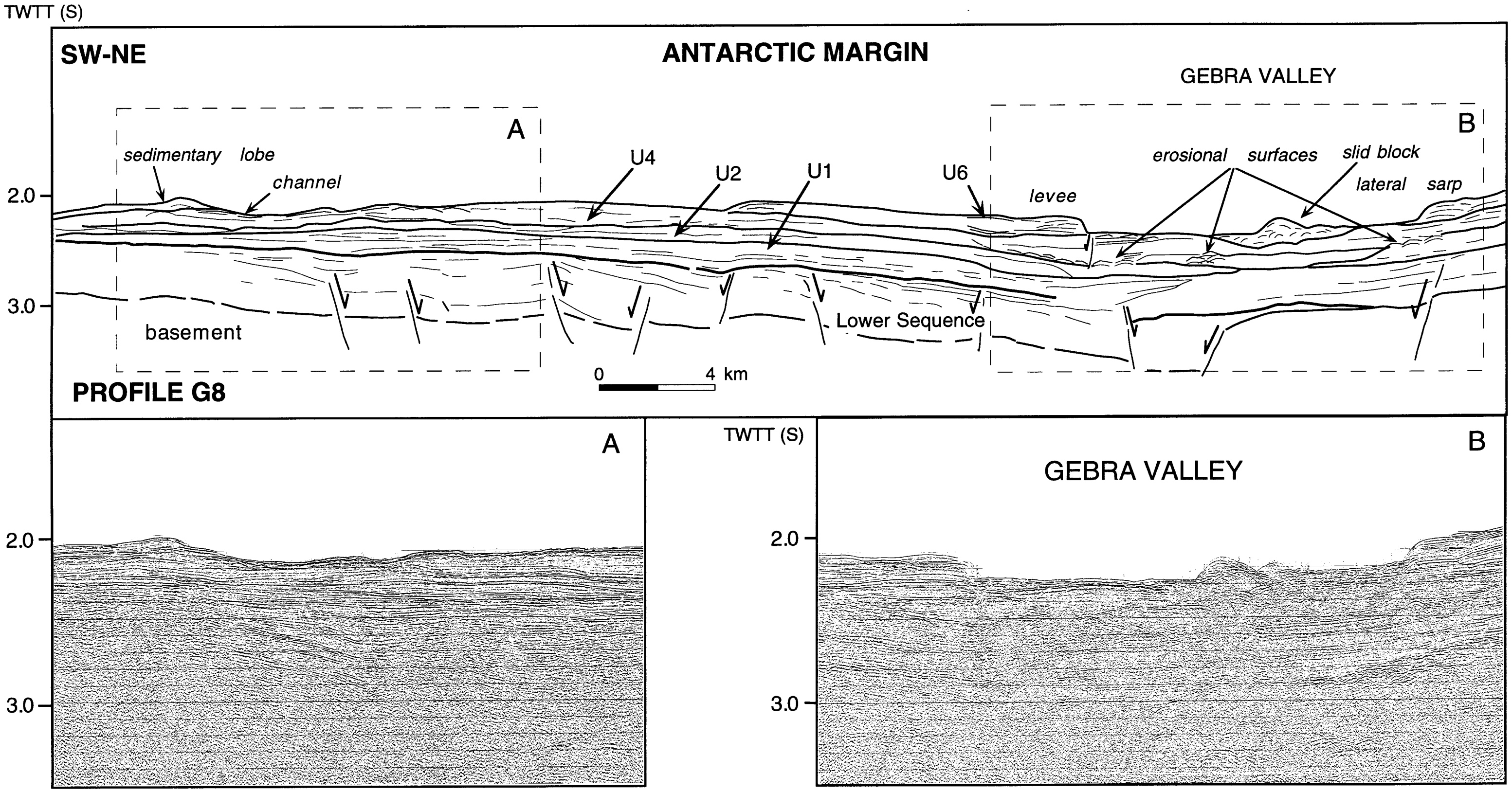

Fig. 7. Interpreted line drawing of seismic line G8 showing the geometry and the distribution of basinal units. Two details of this seismic line show the undulated and chaotic seismic facies at the foot of the Antarctic Peninsula slope. Location of the seismic line in Fig. 1b.

between the AP margin and the volcanic lineament, where it downlaps the basement. The seismic facies of this lower subunit is continuous, parallel and stratified with abundant interstratified seismically chaotic bodies (Fig. 7). The upper subunit occupies the whole basin floor and onlaps the underlying units. It mainly shows a continuous, planar stratified seismic facies (Fig. 7) that changes to a discontinuous subparallel stratified facies in the northern subbasin and King George Basin. The contact between these subunits is a conformable surface with the exception of King George Basin, where the upper subunit onlaps onto the lower one. Lens-shaped bodies with chaotic seismic facies appear locally within the U4 upper subunit and at its top in the northern subbasin (Fig. 6). From their seismic characteristics, we interpreted these as sills intruded through fractures into the sediments (Fig. 6). The thickness of U4 changes markedly along an across-basin section. The maximum thickness, which is around 0.35 s TWTT, occurs at the base of the SSI margin and in King George Basin. In the remaining basin the mean thickness is about 0.15 s TWTT, except at the Gebra Valley where U4 decreases to only 0.05 s TWTT (Fig. 7).

Unit 6 (U6) covers the whole basin floor lying either over U5, as in the southernmost sector of the AP margin, or over U4, as in the rest of the basin. The base of the unit is a conformable subhorizontal surface. In King George Basin, sediments fill and onlap onto the irregular geometry of the depocentre. The top of the unit coincides with the seafloor in a large area at the base of the AP margin, where it often shows an erosional character (Fig. 7). The unit has a characteristic continuous parallel stratified seismic facies and contains interstratified chaotic bodies near the foot of the AP slope (Fig. 3). In the central sector, mounded and tabular bodies with subparallel stratified seismic facies form the sea floor relief up to 150 m, which is highlighted in the swath bathymetry data (Fig. 7). The present-day Gebra Valley is located over U6. The maximum thickness of U6 is 0.2 s TWTT in King George Basin, and it thins and pinches out towards the margins.

Unit 8 (U8) is the youngest basinal seismic unit in the CBB and is uniformly distributed on the basin floor (Figs. 3 and 4). In the southernmost sector it overlies U7 (Fig. 4) while in the rest of the basin it overlies U6 (Figs. 3 and 6). The base of the unit is a conformable surface that onlaps U6. The top of U8 forms the seafloor and locally has erosional truncations (Fig. 7). A continuous parallel stratified seismic facies with high continuity and amplitude reflectors characterises this unit. In the vicinity of the seamounts, this seismic facies gradually changes to a more chaotic facies, which could be attributed to the presence of volcanic material (Fig. 3). Modifications to the dominant seismic facies also occur in the vicinity of the AP margin, where reflectors locally show undulating morphology (Fig. 7). The geometry of U8 is lens-shaped, with the thickest section following the basin axis. The thickness is less than 0.1 s TWTT except for a 4 km wide graben at the foot of the SSI slope, in the central sector, where the thickness reaches 0.15 s TWTT (Figs. 3 and 4).

7. Depositional growth patterns in Central Bransfield Basin

The depositional growth pattern of the AP margin is characterised by stacking of the LS and the slope units U1, U3, U5 and U7 of the Upper Sequence. The SSI margin is characterised by stacking of slope units U3, U5 and U7. The LS is faulted and folded throughout the CBB. It fills and smooths the irregular basement morphology and displays mainly an aggradational configuration. Within the US, U1 has a distinct progradational internal structure, indicating that the AP margin underwent significant progradation during the time of deposition of U1 (Figs. 3 and 4). In contrast, U3, U5 and U7 in the AP, essentially show an aggradational growth pattern with only a subtle internal progradational configuration (Fig. 3). Nevertheless, facing of Orleans Trough, in the southwestern segment of the AP margin, the growth pattern is locally progradational as suggested by the basinward advance of the platform-break (3.5 km) during the deposition of U5 and U7 (Fig. 4).

The basin floor is composed of four vertically stacked, aggrading seismic units U2, U4, U6 and U8, separated by erosional unconformities. These units interfinger with the slope units at the base of the AP and SSI slopes (Fig. 3). Locally, as in King George Basin, the basin-floor sedimentary package can be subdivided into two sections. The lower section (composed of U2 and part of U4) is attached to the AP margin. The upper section (composed of the upper part of U4, U6 and U8) occupies the whole basin floor, onlaps the underlying units and has a clearly aggradational growth pattern.

8. Discussion

The seismic-stratigraphic analysis of the CBB indicates that the sedimentary history of this basin comprises two clearly distinct stages corresponding to the formation of the LS and US. The regional unconformity dividing the two sequences and their differentiated stratal patterns suggest a major change in the style in which the CBB was filled (Fig. 7). We discuss two sedimentary scenarios. The first explains the formation of the LS, which appears to have been mainly conditioned by the initial structural development of the CBB. The second scenario refers to the formation of the US, whose deposition has been mainly governed by the growth and decay of the ice sheets and therefore by glacio-marine sedimentation processes.

8.1. Formation of the Lower Sequence

Deposition of the LS began with the initial fragmentation, rotation, subsidence and extension of continental basement blocks, prior to the onset of seafloor spreading. In fact, the LS would correspond to the ‘rift sequence’ associated with the stretching and rifting stages of the Antarctic continent by Gamboa and Maldonado (1990). The deposition of the units forming the LS was induced by the creation of accommodation space in response to extensional tectonic activity in the incipient CBB (Prieto et al., 1998). Tectonism and subsidence controlled the distribution of sediments in the newly formed basin, as well as synsedimentary deformation of the deposits. Sedimentation of the LS took place in a narrow graben, presently situated beneath the AP margin (Prieto et al., 1998) (Fig. 3). Significant synsedimentary deformation is suggested by the divergent stratified seismic facies occurring in association with normal faults (Fig. 7), and by locally landward-dipping configurations related to the rotation of faulted basement blocks (Fig. 3).

8.2. Formation of the Upper Sequence

The identification within the US of two types of seismic units with different physiographic locations (slope and basinal units), and the interfingering pattern at the base of the AP and SSI margins (Fig. 3), suggest that the US responds to a cyclic depositional pattern (Jeffers and Anderson, 1990). Their setting (offshore glaciated landmasses) and the observed seismic facies (internal stratal pattern and sedimentary architecture) suggest that these units have been deposited by glacio-marine sedimentary processes. Most glacio-marine depositional models based upon seismic stratigraphy (e.g. Larter and Barker, 1989; Jeffers and Anderson, 1990; Cooper et al., 1991; Larter and Cunningham, 1993; Bart and Anderson, 1996) do involve a strong cyclicity that is attributed to the alternation of periods of advance and retreat over the shelf of the ice sheets covering the glaciated continents.

Our interpretation is, that the CBB slope units were deposited during glacial periods, when the ice sheets expanded and advanced over the margin (Fig. 8). Such an interpretation agrees with the generally accepted glacio-marine sedimentation models (e.g. Larter and Barker, 1989; Jeffers and Anderson, 1990; Cooper et al., 1991; Larter and Cunningham, 1993; Larter and Vanneste, 1995; Bart and Anderson, 1996). The development of the CBB basinal units should, therefore, have taken place at the end of glacial periods and during interglacial periods, when the ice sheets retreated (Fig. 9). During this latter phase, the shelf and the upper slope were mainly characterised by sediment starvation, depositional by-pass and erosion (Vorren et al., 1989; Henrich, 1990; Bart and Anderson, 1996).

8.2.1. Slope units

The seismic configuration of the slope units (U1, U3, U5 and U7) suggests that they were formed when the ice sheets expanded and advanced onto the AP and SSI margins. An advancing ice sheet produces severe erosion of the existing sea-floor strata, and the eroded material is mainly transported subglacially at the base of the ice sheet (Fig. 8), before finally being deposited at the moving ice-sheet grounding line. Eventually, the advance of the grounding line to the platform break causes the

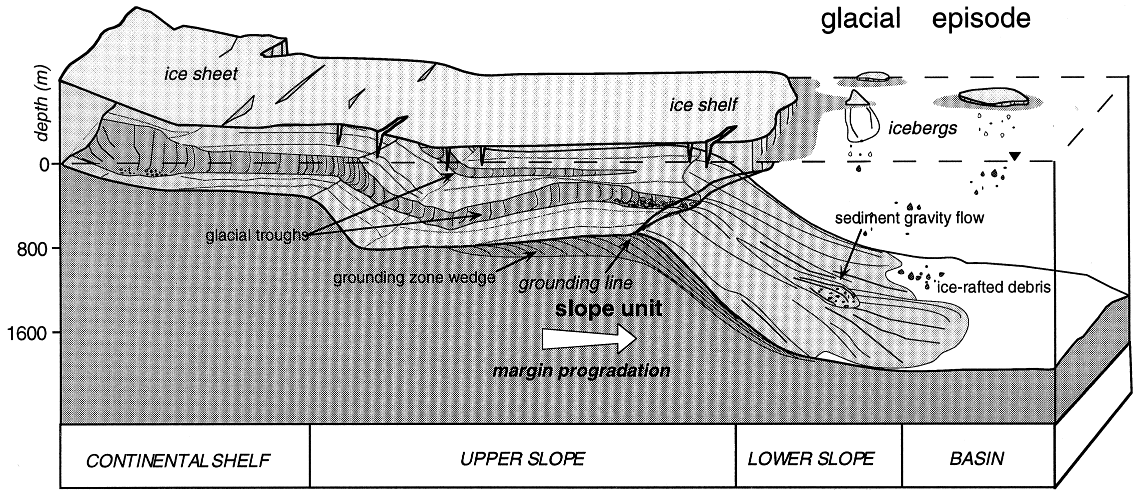

Fig. 8. Sedimentary model showing the subglacial erosion and deposition during a glacial episode where the front of the ice sheet reaches the shelf edge. The result is the formation of a large sedimentary prograding wedge developed from the upper platform to the base of the slope.

glacial debris to be deposited beyond the platform edge and be transported further downslope by gravity-driven processes (gravity and mass-flow) (Powell, 1984), thereby contributing to the oversteepening of the slope (Larter and Barker, 1989; Larter and Cunningham, 1993) and to the development of downlapping stratified slope units with a predominance of proximal debris flow deposits. These processes end with the formation of a prograding sedimentary wedge with downlapping foresets similar to those geometries described by Bart and Anderson (1995) and known as grounding zone wedge (Fig. 8).

The strong erosion associated with the advancing ice sheets may have created the widespread truncation surfaces that bound the top of each seismic unit. The size and volume of each slope unit in the AP margin, as well as their internal configuration, are probably controlled by the duration and inten-

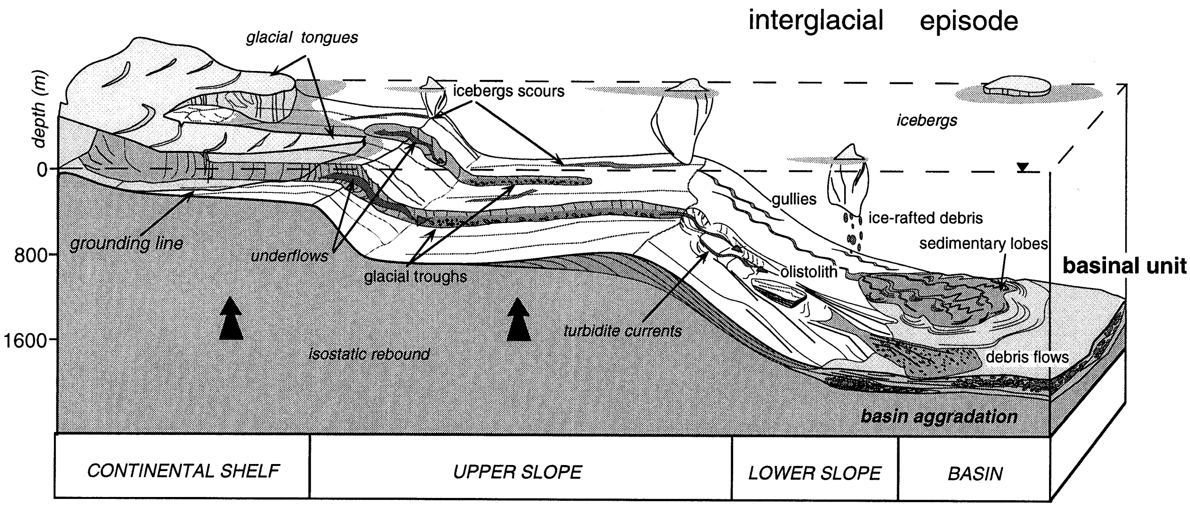

Fig. 9. Model showing the sedimentary processes during a glacial retreat. At the upper platform the erosion and sediment by-pass predominate over sedimentation. Slope instabilities and subglacially-generated marine currents rework and redistribute sediments initially deposited on the platform.

sity of the glacial period (Bart and Anderson, 1995; Vanneste et al., 1995; Kuvaas and Kristoffersen, 1996). The velocity of the advance, the maximum extension and the permanence of the ice sheets over the margin are, hence, the key factors. The glacial period with the largest magnitude and duration presumably corresponds to the deposition of U1, as suggested by the great extent of this unit (thickness of 0.25–0.35 s TWTT), and also by its relatively high-angle (10º) progradational foresets on the upper platform (Figs. 3 and 4). In contrast, the glacial periods that led to the deposition of U3, U5 and U7 must have been of much smaller magnitudes and duration, as suggested by their reduced dimensions (thickness from 0.15 to 0.2 ms), and by only subtle evidence of progradation on the upper platform (Figs. 3 and 4). Comparable changes in the internal configuration of slope strata observed along other segments of the Antarctic margins have been attributed to the high-frequency sea-level fluctuations of the Plio–Pleistocene which would have limited the duration of grounding events on the shelf (Anderson et al., 1991; Bartek et al., 1991; Alonso et al., 1992).

The variable seaward extension and basinward progradation of each individual slope unit along the AP margin can be attributed to the uneven volumes of sediment supplied to the margin by the ice sheet. The strongest progradation occurs in an area facing the Orleans Trough, indicating that this trough is a dominant sediment source for the AP margin. The highest progradational advances (3.5 km, from U5 to U7) have been identified offshore from that through (Fig. 4). This probably was a thicker and faster-moving ice stream with enhanced transport efficiency with respect to adjacent segments of the ice sheet. Similar point-source transport and deposition has been suggested to explain the variable extent of seismic units in the NW Antarctica Peninsula continental shelf (Bart and Anderson, 1996). Variations in the seismic configuration within the slope units, such as minor internal unconformities, have been identified in front of Orleans Trough (Fig. 4). We attribute them to short-lived stabilisations or retreats of the grounding line during a main glacial episode which might have been combined with local shifts of the transport and depositional pathways. This would confirm the idea that it is the mouth of a glacial trough where the most complete and detailed sedimentary record of the glacial advances is contained (Bart and Anderson, 1996).

The mounded landward-dipping body within U7 (Fig. 3) was previously observed by Banfield and Anderson (1995), who interpreted it as diamicton deposits which had developed beneath the ice sheet close to the grounding line. Such a grounding zone moraine would indicate the maximum extent reached by the ice sheet during the last glacial advance recorded in this segment of the AP upper platform. In this setting, the prograding sedimentary wedge of U7 would have been deposited seaward from that grounding zone (Fig. 3), and would consist mainly of glacio-marine and sediment gravity flow deposits, reworked by marine currents and probably by meltwater streams in a proglacial environment. The isolated landward- dipping mounded body of U7 is, however, a local feature. During the time of its deposition the grounding line possibly advanced to the platform edge in most of the AP margin segments, such as the Orleans Trough segment, where ice feed was greatest.

The preservation and lateral continuity of the slope units in the CBB were probably strongly controlled by subsidence and isostatic depression produced by extensional tectonism and ice-sheet loading, respectively. There are no data about subsidence values in the CBB, although in a recent study on the geodynamic evolution of the CBB Gràcia et al. (1996) claimed a significant rate of subsidence during the opening of the basin and the formation of the LS, which probably continued during the sedimentation of the US.

8.2.2. Basinal units

The seismic features of the basinal units (U2, U4, U6 and U8), with chaotic interstratified and undulating stratified facies at the foot of the slopes, changing to a planar continuous facies on the central basin floor (Figs. 3 and 7), suggest that these units are mainly generated by downslope depositional processes, such as mass gravity flows, slumps, turbidity currents and gravitational instabilities (Drewy and Cooper, 1981; Wright and Anderson, 1982; Kuvaas and Kristoffersen, 1996). The result of these processes are the Gebra Valley, small gullies and deposits, such as the channels and levees forming the poorly developed depositional fanlobe at the foot of the AP slope (Figs. 7 and 10).

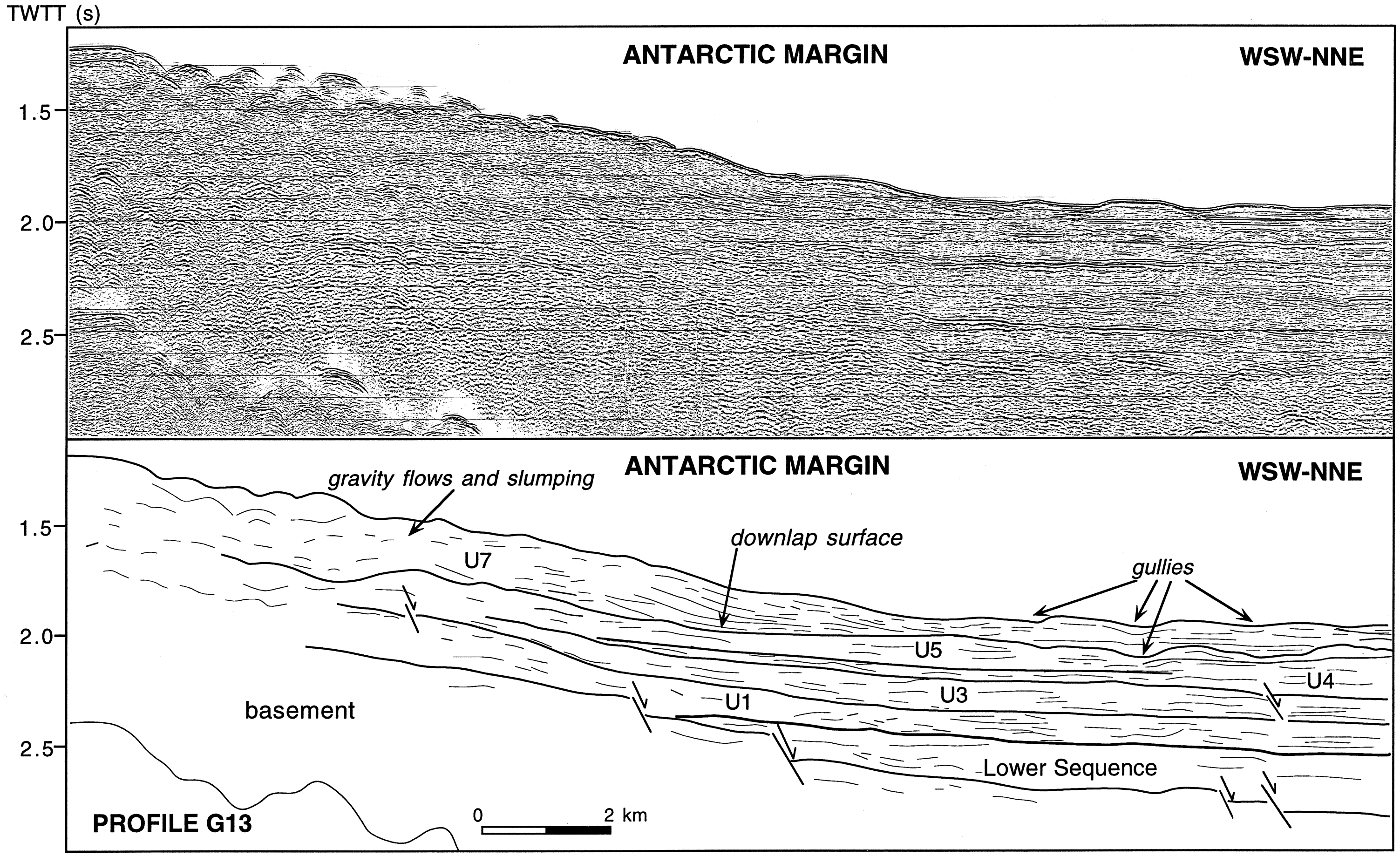

Fig. 10. Seismic line G13 and interpreted line drawing showing the geometry of U7 and the channels and gullies eroded in the slope. Location of the seismic line in Fig. 1b.

These processes probably began at the end of glacial periods, when large volumes of sediment deposited on the slope during ice-sheet advance became unstable (Fig. 9). Several studies (Aksu and Hiscott, 1989; Henrich, 1990; Syvitski et al., 1996) have demonstrated that sediments that are initially deposited on a steep slope are subsequently removed and redeposited on the basin floor via turbidity currents. Moreover, the glacio-isostatic rebound produced by the retreat of the ice sheets would probably also have produced instabilities big enough to generate mass movements of varying magnitudes, as suggested by Bart et al. (1998) (Fig. 9). The role of gravity flows in the formation of the CBB basinal units during interglacials has also been demonstrated by means of detailed sediment core studies, which identified small-scale turbidite sequences (Fabrés et al., 1997). We, therefore, propose that the basinal units of the CBB were deposited after the glacial maxima and during periods of ice-sheet retreat.

After the main phases of glacial advance in the AP margin, the transfer of sediments to the basin floor seems to have occurred through the Orleans Trough, the Antarctic Sound and the two smaller glacial troughs which lie in between (Figs. 2 and 9). In this set of troughs, ice sheets and ice streams clearly reached their maximum thickness during glaciation, but ice tongues probably lasted longer than in the open unconstrained shelf and continued to occupy the troughs long after the start of the ice retreat. Some glacial ice might even have lasted until the total disintegration of the ice sheet. In such a setting, ice-tongues would have continued to promote active sediment transport and release to the margin and deep basin (Fig. 9). A particularly significant role might have been played by turbidity currents generated by sediment-laden subglacial meltwater (Henrich, 1990). These currents would have been able to excavate gullies downslope (Vorren et al., 1989; Kuvaas and Kristoffersen, 1991), such as those identified in front of the Orleans Trough and the AP margin (Figs. 2 and 10). Due to the longer exposure of glacial troughs and channels to subglacial conditions, turbidity currents would have remained active for a longer time in these areas. Such conditions would have concluded with the complete disintegration of the ice tongues and, eventually, the infilling of the less active troughs.

The basinal units also contain sediments from sources in the SSI margin. During interglacial periods, terrigenous materials, mainly from the fjords in the SSI, were transported basinward by melt water plumes and turbidity currents (Jeffers and Anderson, 1990). Despite the relatively smaller size of the SSI drainage area (Domack and Ishman, 1993) and, consequently, the faster decay of ice sheets, at this point the SSI margin seems to have delivered a comparatively large amount of sediment to the CBB (Jeffers and Anderson, 1990). This observation is also supported by our data set, where a rather thick (0.7 s TWTT) sedimentary cover is trapped in the northern subbasin, behind the sedimentary barrier formed there by the axial volcanic lineament. The large volume of sediment coming from the SSI margin has been attributed to the warmer conditions of the ice sheet covering the SSI, to high rates of meltwater production (Griffith and Anderson, 1989), to oceanographic and physiographic characteristics of the margin and bays and to the more easily eroded volcaniclastic source (Domack and Ishman, 1993).

Ice-rafted debris derived from calved icebergs (Henrich, 1990), and pelagic and hemipelagic particles from gravitational settling (Banfield and Anderson, 1995) are also produced by the set of processes that contributed to the formation of the basinal units. Nevertheless, pelagic or hemipelagic components probably represent only a small proportion of each basinal unit (Yoon et al., 1994), as suggested by the irregular distribution of these units and their variable thickness along and across the basin.

The irregular distribution of the basinal units was also influenced by volcanic and tectonic factors, such as the growth of volcanic edifices and the presence of basement highs during their deposition. This could explain the differential distribution displayed by U2 and part of U4, which are restricted to the southern subbasin, compared to that of U6 and U8 basinal units that occupy the whole basin floor.

9. Conclusions

The seismic-stratigraphic analysis of high-resolution seismic records from the CBB allows us to identify two sedimentary sequences: a faulted, folded Lower Sequence, and an almost undeformed Upper

Sequence. Tectonic activity, related to the first stage of extension and opening of CBB, was responsible for the observed stratal patterns, synsedimentary deformation and spatial distribution of the Lower Sequence. This sequence was deposited in a graben presently situated below the AP margin. In contrast, tectonism played only a minor role in the formation of the Upper Sequence. Stratal pattern within this sequence were mainly controlled by the advance and retreat of ice sheets during glacial cycles.

The successive advance and retreat of the ice sheet over the margin, produced a cyclical sedimentation pattern. The formation of slope units (U1, U3, U5 and U7) in the AP and SSI margins occurred during glacial periods, and the development of basinal units (U2, U4, U6 and U8) occurred during ice-sheet retreats at the end of glacial periods and during interglacial periods. This cyclical pattern did not change significantly during the time of sedimentation of the Upper Sequence. The sedimentary growth pattern of the slope units was progradational during U1 and mainly aggradational during the deposition of U3 to U7. This change from progradational to aggradational growth of the margin was mainly controlled by the duration of glacial periods. Variations in sediment supply related to the presence of ice streams controlled the non-uniform progradation of each slope unit during the associated glacial period in the AP margin. The sedimentary growth pattern of the basinal units is aggradational.

Geodynamic and tectonic evolution of the CBB partially conditioned the deposition of the Lower Sequence and Upper Sequence in various ways (Prieto et al., 1998). First, the absence of the Lower Sequence and U1 in the SSI margin was probably due to a later development of this margin at the time of deposition. Consequently, there was no accommodation space to deposit these units. Second, tectonic subsidence favoured the preservation of slope units in the AP and SSI margins. Third, and finally, tectonism determined the structural framework of the basin and therefore the distribution of basinal units (Prieto et al., 1998).

Acknowledgements

We cordially thank the captain of the R/V *Hespérides*, Commandant V. Quiroga, and the crew members who participated in the Gebra 93 cruise. We thank M. Farrán and J. Sorribas for processing the swath-bathymetry data. We would also like to thank E.W. Domack, J.B. Anderson and the editor, whose comments and suggestions have greatly improved the article. This work was supported by the Spanish 'Programa Nacional de Investigación en la Antártida', project ANT-93-1008-C03-01, funded by the CICYT. The GRC Geociències Marines at the University of Barcelona has been supported by 'Generalitat de Catalunya' grant GRC 94/95-1026. M.J. Prieto benefited from a fellowship from the 'Universitat de Barcelona' (CPI-16), and M. de Batist is senior research assistant of the FWO Vlaanderen. The participation of the University of Gent (Belgium) in the Gebra 93 cruise was supported by the Belgian Program of Antarctic Research Programme, project A3-02-002.

References

Acosta, J., Herranz, P., Sanz, J.L., Uchupi, E., 1992. Antarctic continental margin: Geologic image of the Bransfield Trough, an incipient ocean basin. In: Poag, C.W., Graciansky, P.C. (Eds.), Geologic Evolution of Atlantic Continental Rises. Van Nostrand Reinhold, New York, pp. 49–61.

Aitkenhead, N., 1975. The geology of Duse Bay-Larsen inlet area, North-East Graham Land (with particular reference to the Trinity Peninsula Series). BAS Sci. Rep. 51, 62 pp.

Aksu, A.E., Hiscott, R.N., 1989. Slides and debris flows on the high-latitude continental slopes of Baffin Bay. Geology 17, 885–888.

Alonso, B., Anderson, J.B., Díaz, J.I., Bartek, L.R., 1992. Pliocene–Pleistocene seismic stratigraphy of the Ross Sea: Evidence for multiple ice sheet grounding episodes. Antarct. Res. Ser. (Contrib. Antarct. Res. III) 57, 93–103.

Anderson, J.B., Kurtz, D.D., Domack, E.W., Balshaw, K.M., 1983. Development of a polar glacial-marine sedimentation model from Antarctic Quaternary deposits and glaciological information. In: Molnia, B.F. (Ed.), Glacial-Marine Sedimentation. Plennum Press, New York, pp. 629–666.

Anderson, J.B., Bartek, L.R., Thomas, M.A., 1991. Seismic and sedimentological record of glacial events on the Antarctic Peninsula shelf. In: Thomson, M.R.A., Crame, J.A., Thomson, J.W. (Eds.), Evolution of Antarctica. Cambridge University Press, Cambridge, pp. 687–691.

Ashcroft, W.A., 1972. Crustal structure of the South Shetland Islands and Bransfield Strait. BAS Sci. Rep. 66, 43 pp.

Banfield, L., Anderson, J.B., 1995. Seismic facies investigation of the Late Quaternary glacial history of Bransfield Basin, Antarctica. In: Cooper, A.K., Barker, P.F., Brancolini, G.

(Eds.), Geology and Seismic Stratigraphy of the Antarctic Margin. Am. Geophys. Union, Antarct. Res. Ser. 68, 123–140.

Barker, D.H.N., Austin, J.A., 1994. Crustal diapirism in Bransfield Strait, West Antarctica. Evidence for distributed extension in marginal basin formation. Geology 22, 657–660.

Barker, D.H.N., Austin, J.A., 1995. Characterization of acoustic basement, Bransfield Strait: Implications for geologic evolution of this marginal basin. Abstr. VII Int. Symp. Antarct. Earth Sci. (ISAES), p. 20.

Barker, P.F., 1982. The Cenozoic subduction history of the Pacific margin of the Antarctic Peninsula: Ridge crest-trench interactions. J. Geol. Soc. London 139, 787–801.

Barker, P.F., Dalziel, I.W.D., 1983. Progress in geodynamics of the Scotia Arc region. In: Cabré, R. (Ed.), Geodynamics of the Eastern Pacific Region, Caribbean and Scotia Arcs. AGU Geodyn. Ser. 9, 137-170.

Bart, P.J., Anderson, J.B., 1995. Seismic record of glacial events affecting the Pacific margin of the Northwestern Antarctic Peninsula. In: Cooper, A.K., Barker, P.F., Brancolini, G. (Eds.), Geology and Seismic Stratigraphy of the Antarctic Margin. AGU Antarct. Res. Ser. 68, 74-95.

Bart, P.J., Anderson, J.B., 1996. Seismic expression of depositional sequences associated with expansion and contraction of ice sheets on the northwestern Antarctic Peninsula continental shelf. In: De Batist, M., Jacobs, P. (Eds.), Geology of Siliciclastic Continental Shelves Seas. Geol. Soc. London Spec. Publ. 117, 171-186.

Bart, P.J., De Batist, M., Jokat, W., 1998. Interglacial collapse of Crary Trough Mouth Fan, Weddell Sea, Antarctica: implications to high-latitude sequence stratigraphy. J. Sediment. Res., submitted.

Bartek, L.R., Vail, P.R., Anderson, J.B., Emmet, P.A., Wu, S., 1991. Effect of Cenozoic ice sheet fluctuations in Antarctica on the Stratigraphic Signature of the Neogene. J. Geophys. Res. 96, 6753–6778.

Birkenmajer, K., 1992. Evolution of the Bransfield Basin and Rift, West Antarctica. In: Yoshida, Y., Kamimura, K., Shiraishi, K. (Eds.), Recent Progress in Antarctica, Earth Science. Terra Scientific Publ., Tokio, pp. 405–410.

Canals, M., Acosta, J., Baraza, J., Bart, P., Calafat, A.M., Casamor, J.L., De Batist, M., Ercilla, G., Farrán, M., Francés, G., Gràcia, E., Ramos-Guerrero, E., Sanz, J.L., Sorribas, J., Tassone, A., 1994. La Cuenca Central de Bransfield (NW de la Península Antártica): Primeros resultados de la Campaña Gebra 93. Geogaceta 16, 132–135.

Cooper, A.K., Barret, P.J., Hinz, K., Traube, V., Leitchenkov, G., Stagg, H., 1991. Cenozoic prograding sequences of the Antarctic continental margin: a record of glacio-eustatic and tectonic events. Mar. Geol. 102, 175–213.

Domack, E.W., Ishman, S., 1993. Oceanographic and physiographic controls on modern sedimentation within Antarctic fjords. Geol. Soc. Am. Bull. 105, 1175–1189.

Drewy, D.J., Cooper, A.P.R., 1981. Processes and models of Antarctic glaciomarine sedimentation. Ann. Glaciol. 2, 117–122.

Fabrés, J., Calafat, A., Canals, M., Francés, G., Bárcena, M.A., Ledesma, S., Flores, J.A., 1997. Identificación de procesos sedimentarios en la Cuenca Central de Bransfield (Antàrtida): estudio preliminar de las características sedimentológicas y composición elemental (C, Si) de los sedimentos recientes. Real Soc. Esp. Hist. Nat. 93 (1234), 83–92.

Fisk, M.R., 1990. Volcanism in the Bransfield Strait, Antarctica. J. S. Am. Earth Sci. 3, 91–101.

Gamboa, L.A.P., Maldonado, P.R., 1990. Geophysical investigations in the Bransfield Strait and in the Bellingshausen Sea — Antarctica. In: John, B.St. (Ed.), Antarctica as an Exploration Frontier: Hydrocarbon Potential Geology and Hazards. AAPG Stud. Geol. 31, 127-141.

Garret, S.W., 1990. Interpretation of reconnaissance gravity and areomagnetic surveys of the Antarctic Peninsula. J. Geophys. Res. 95, 6759–6777.

Gràcia, E., Canals, M., Farràn, M., Prieto, M.J., Sorribas, J., Gebra Team, 1996. Morphostructure and evolution of the Central and Eastern Bransfield Basins (NW Antarctic). Mar. Geophys. Res. 18 (123), 429–448.

Gràcia, E., Canals, M., Farràn, M., Sorribas, J., Pallàs, R., 1997. The Central and Eastern Bransfield basins (Antarctica) from high-resolution swath-bathymetry data. Antarct. Sci. 9 (2), 168–180.

Grad, M., Guterch, A., Sroda, P., 1992. Upper crustal structure of Deception Island area, Bransfield Strait, West Antarctica. Antarct. Sci. 4, 469–476.

Griffith, T., Anderson, J.B., 1989. Climatic control of sedimentation in bays and fjords of the northern Antarctic Peninsula. Mar. Geol. 85, 181–204.

Henrich, R., 1990. Cycles, rhythms, and events in Quarternary Artic and Antarctic glaciomarine deposits. In: Bleil, U., Thiede, J. (Eds.), Geological History of the Polar Oceans: Arctic versus Antarctic. Kluwer, Dordrecht, pp. 213–244.

Henriet, J.P., Meissner, R., Miller, H., Grape Team, 1992. Active margin processes along Antarctic Peninsula. Tectonophysics 201, 1–25.

Hyden, G., Tanner, W.G., 1981. Late Paleozoic–Early Mesozoic fore-arc basin sedimentary rocks at the Pacific Margin in Western Antarctica. Geol. Rundsch. 70, 529–541.

Jeffers, J.D., Anderson, J.B., 1990. Sequence stratigraphy of the Bransfield Basin, Antarctica. Implications for tectonic history and hydrocarbon potential. In: John, B.St. (Ed.), Antarctica as an Exploration Frontier: Hydrocarbon Potential Geology and Hazards. AAPG Stud. Geol. 31, 13-30.

Kuvaas, B., Kristoffersen, Y., 1991. The Crary Fan: a trough-mouth fan on the Wedell Sea continental margin, Antarctica. Mar. Geol. 97, 345–362.

Kuvaas, B., Kristoffersen, Y., 1996. Mass movements in glaciomarine sediments on the Barents Sea continental slope. Global Planet. Change 12 (1234), 287–307.

Larter, R.D., Barker, P.F., 1989. Seismic stratigraphy of the Antarctic Peninsula margin: A record of Pliocene–Pleistocene ice volume and paleoclimate. Geology 17, 731–734.

Larter, R.D., Cunningham, A.P., 1993. The depositional pattern and distribution of glacial–interglacial sequences on the Antarctic Peninsula Pacific margin. Mar. Geol. 109, 203–219.

Larter, R.D., Vanneste, L.E., 1995. Relict subglacial deltas on the Antarctic Peninsula outer shelf. Geology 23 (1), 33–46.

Lawver, L.A., Keller, R.A., Fisk, M.R., Strelin, J., 1995. Bransfield Strait, Antarctic Peninsula: Active extension behind a dead arc. In: Taylor, B. (Ed.), Back-arc Basins: Tectonics and Magmatism. Plenum, New York, pp. 315–342.

Lawver, L.A., Ghidella, M., Von Herzen, R.P., Keller, R., 1996. Distributed, active extension in Bransfield Basin, Antarctic Peninsula: evidence from multibeam bathymetry. GSA Today 6 (11), 1–6.

Nagihara, S., Lawver, L.A., 1989. Heat flow measurements in the King George Basin, Bransfield Strait. Antarct. J. Sci. 23, 123–125.

Pelayo, A.M., Wiens, D.A., 1989. Seismotectonics and relative plate motions in the Scotia Sea region. J. Geophys. Res. 94, 7293–7320.

Powell, R.D., 1984. A model for sedimentation by tidewater glaciers. Ann. Glaciol. 2, 129–134.

Prieto, M.J., Gràcia, E., Canals, M., Ercilla, G., De Batist, M., 1997. Sedimentary history of the Central Bransfield Basin (NW Antarctic Peninsula). In: Ricci, C.A. (Ed.), The Antarctic Region: Geological Evolution and Processes. Proc. VII ISAES. Terra Antarctica Publ., Siena, pp. 711–717.

Prieto, M.J., Canals, M., Ercilla, G., De Batist, M., 1998. Structure and geodynamic evolution of Central Bransfield Basin (NW Antarctica) from seismic reflection data. Mar. Geol. 149 (1234), 17–38.

Roach, P.J., 1978. The nature of back-arc extension in Bransfield Strait. Geophys. J. R. Astron. Soc. 53, 165.

Saunders, A.D., Tarney, J., 1984. Geochemical characteristics of basaltic volcanism within backarc basins. In: Kokelaar, B.P., Howells, M.F. (Eds.), Marginal Basin Geology: Volcanism and Associated Sedimentary and Tectonic Proceses in Modern and Ancient Marginal Basins. Geol. Soc. London Spec. Publ. 16, 59-76.

Smellie, J.L., Pankhurst, R.J., Thomson, M.R.A., Davies, R.E.S., 1984. The Geology of the South Shetland Islands: VI Stratigraphy, Geochemistry and Evolution. BAS Sci. Rep. 87, 85 pp.

Syvitski, J.P.M., Andrew, J.T., Dowdeswell, J.A., 1996. Sediment deposition in an iceberg-dominated glacimarine environment, East Greenland: basin fill implications. Global Planet. Change 12 (1234), 251–270.

Vanneste, K., Uenzelmann-Neben, G., Miller, H., 1995. Seismic evidence for long-term history of glaciation on central East Greenland shelf south of Scoresby Sund. Geo-Mar. Lett. 15, 63–70.

Vorren, T.O., Lebesbye, E., Andreassen, K., Larsen, K.B., 1989. Glacigenic sediments on a passive continental margin as exemplified by the Barents Sea. Mar. Geol. 85, 251–272.

Wright, R., Anderson, J.B., 1982. The importance of sediment gravity flow to sediment transport and sorting in a glacial marine environment: Eastern Weddell Sea, Antarctica. Geol. Soc. Am. Bull. 93, 951–963.

Yoon, H.I., Han, M.W., Park, B.K., Oh, J.K., Chang, S.K., 1994. Depositional environment of near-surface sediments, King George Basin, Brasfield Strait, Antarctica. Geo-Mar. Lett. 14, 1–9.